

Electronic stopping calculated using explicit phase shift factors

J. Sillanpää,* J. Peltola, K. Nordlund, and J. Keinonen
Accelerator Laboratory, P.O. Box 43, FIN-00014 University of Helsinki, Finland

M. J. Puska

Laboratory of Physics, Helsinki University of Technology, P.O. Box 1100, FIN-02015 HUT, Finland

(Received 2 November 2000; published 15 March 2001)

Predicting range profiles of low-energy (0.1–10 keV/amu) ions implanted in materials is a long-standing problem of considerable theoretical and practical interest. We combine here the best available method for treating the nuclear slowing down, namely a molecular-dynamics range calculation method, with a method based on density-functional theory to calculate electronic slowing down for each ion-target atom pair separately. Calculation of range profiles of technologically important dopants in Si shows that the method is of comparable accuracy to previous methods for B, P, and As implantation of Si, and clearly more accurate for Al implantation of Si.

DOI: 10.1103/PhysRevB.63.134113

PACS number(s): 61.72.Tt, 34.50.Bw, 34.10.+x

Calculating the force which slows down energetic ions traversing in materials (the stopping power) is a long-standing problem of considerable theoretical and practical interest.^{1–3} While the stopping power caused by collisions between an ion and atoms can now be predicted very accurately,^{4–6} there is still uncertainty in how the stopping caused by collisions between an ion and electrons (electronic stopping) should be calculated for ion velocities below the Bohr velocity (namely at energies of the order of 0.1–10 keV/amu). This is an especially pressing problem for obtaining range profiles for dopants implanted in crystal channel directions in semiconductors, since on one hand the uncertainties are particularly large in this case and on the other hand this case is important for the microelectronics industry.

The most common approach for obtaining stopping powers is to first derive a stopping power for a proton in a material, and then use a scaling law to obtain the stopping power of heavier ions. To obtain the stopping power of the proton, the most popular approach is to use models^{7,8} based on the scattering phase shifts for Fermi-surface electrons. The phase shifts are determined within the density-functional theory (DFT) (Ref. 9) for a proton embedded in a homogeneous electron gas.^{10,11} This approach has proven successful for some technologically important ion-target combinations, such as B-Si, P-Si, and As-Si,^{12,5,13} but leads into severe difficulties (a physically unjustified parameter value) for the case of Al-Si.⁵

However, the original model with self-consistently determined phaseshifts offers another, frequently overlooked, approach to obtain stopping powers for heavy ions. Instead of using scaling laws, it is possible to explicitly calculate phase shift factors for any given ion-target atom combinations. The phase shift factors can be calculated directly from DFT, so this approach does not use any empirical or fitted input factors.

Another noteworthy approach to predicting the electronic stopping is the local plasma approximation. However, this model does not presently treat channeling anisotropies in the electron distribution,¹⁴ and hence is not applicable here.

In this paper, we combine the best available simulations methods for calculating ion range profiles with electronic stopping powers derived from realistic three-dimensional charge distributions of the Si lattice and explicit calculation of phase shift factors. We compare the calculation results with a wide range of experimental range profiles for implantation in silicon channels.

The electronic stopping model used in this work is based on the density-functional formalism. Unlike models based on the Brandt-Kitagawa (BK) theory,^{15,16} it takes the structure of the electron cloud of the ion into account and does not employ any scaling laws. The electronic stopping power for a slow ($v < v_F$, where v_F is the Fermi velocity of the electrons of the material) ion in a homogeneous electron gas can be expressed as^{7,8}

$$S = \frac{3v}{k_F r_s^3} \sum_{l=0}^{\infty} (l+1) \sin^2[\delta_l(E_F) - \delta_{l+1}(E_F)], \quad (1)$$

where k_F is the Fermi momentum of electrons of the target, r_s the one-electron radius ($r_s = [3/(4\pi\rho)]^{1/3}$, where ρ is the electron density) and $\delta_l(E_F)$ the phase shift for the scattering of an electron at the Fermi energy.

For a given ion (nuclear charge Z), we determine the phase shifts in Eq. (1) by solving for the self-consistent electronic structure of the atom (ion) embedded in a homogeneous electron gas.¹¹ The nonlinear screening is obtained by the DFT within the local-density approximation for the electron exchange and correlation effects. The screening cloud consists of bound electron states localized near the nucleus and of delocalized scattering states. All the states are solved self-consistently by numerical integration. More specifically, the single-particle Kohn-Sham wave functions corresponding to the delocalized scattering states are solved near the nucleus and matched at a given (large) radius to the asymptotic form of the scattering wave,

$$\cos[\delta_l(k)]j_l(kr) - \sin[\delta_l(k)]n_l(kr), \quad (2)$$

where j_l and n_l are the spherical Bessel and Neuman functions, respectively, and k is the electron wave vector. For the self-consistent potential the phase shifts at the Fermi energy obey the Friedel sum rule

$$\frac{2}{\pi} \sum_l (2l+1) \delta_l(E_F) = Z. \quad (3)$$

It should be noted that the validity of the phase shift approach [Eq. (1)] is limited to ion velocities clearly lower than the Fermi velocity. Then the potential of a static calculation can be used to determine the Fermi level phase shifts and one does not need worry about different ionization states. However, applying Eq. (1) is a subtle question because the phase shifts are determined from the Kohn-Sham electron wave functions which are only auxiliary functions in the formalism.⁹ On the other hand, the low-velocity stopping power is defined via the phase shifts corresponding to the ground state of an atom in a homogeneous electron gas and it is a ground-state property. According to the DFT all the ground-state properties can be calculated exactly as functionals of the ground-state electron density. In practice, when comparing with experiment or better many-body calculations many properties calculated using Kohn-Sham wave functions have turned out to be rather good estimates.

The Fermi level phase shifts are calculated for a regular grid of one-electron radius r_s values. The tabulated values are then used in interpolating the phase shifts for a desired electron density.

In order to describe, e.g., channeling accurately, one has to take the anisotropy of the electron distribution of the material into account. We calculate the three-dimensional charge distribution of silicon using the Dawson-Stewart-Coppens formalism¹⁷⁻²⁰ and the Hartree-Fock wave functions calculated by Clementi and Roetti.²¹ This is an efficient scheme to produce the values of electron density in a huge (128^3) number of grid points. We have compared the values at representative points with those obtained by first-principles DFT methods. We found only relatively small differences and expect therefore that the approximations in the electron density have only minor effects in comparison with other approximations made in our scheme. Using the calculated three-dimensional charge distribution the electronic stopping power is then obtained by employing the idea of local response: the stopping power at a given point depends only on the electron density at that point.

To calculate the range profiles, we used a molecular-dynamics range calculation method,²² which has been described in detail for this stopping model in Ref. 13. We did not include the charge state of the incoming ion in the model, since the original charge state of the ion affects the stopping only in the first few monolayers of the target. After that, the charge state depends only on its velocity.²³

We simulated range profiles in channeling directions for all the cases where we have found experimental data in the literature which lie in the energy regime where the assumption of a velocity-proportional stopping is valid.¹³ We present here representative results (both in terms of good and bad agreement with experiment) for all the cases except H.

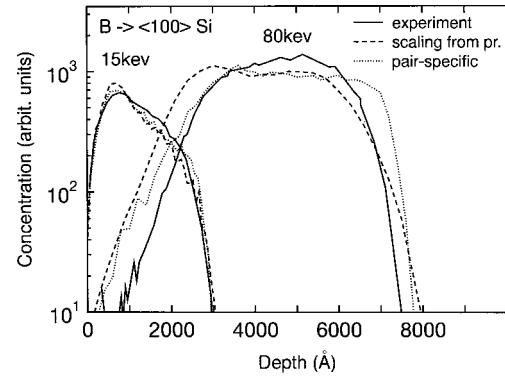


FIG. 1. Simulated and measured ranges of 15-keV and 80-keV B ions in the $\langle 100 \rangle$ channel of silicon. The experimental data was measured with SIMS (Ref. 12).

Results for H implantation in Si have been presented in our earlier paper.¹³ Since they are not affected by scaling laws we do not present them again here.

We compare the results of the model with our earlier model, which is otherwise similar to the present one, except that it used a scaling law based on the Brandt-Kitagawa theory rather than phase shift factors to obtain the stopping of heavy ions, and includes the Firsov model.¹³ We have previously shown that even the use of the scaling law gives much better agreement than the common TRIM/ZBL model,^{24,2} and comparable agreement with the results of other authors,⁵ so we do not repeat these comparisons here. The presented results are grouped by ion-target combination and channeling directions.

For B implantation of Si our pair-specific model gives quite good agreement with experiments in random crystal directions (not shown) and in the $\langle 100 \rangle$ direction (Fig. 1), as does the previous scaling law model. In the $\langle 110 \rangle$ direction (Fig. 2) both models clearly overestimate the ranges. But the shape of the curve for the pair-specific model is closer to the experimental curve. The likely reason to the remaining discrepancy is that r_s is obtained for a pointlike atom, and a charge-averaging scheme should be used to account for the size of the ion.¹³

Obtaining accurate range profiles for Al implanted into channeling directions in Si has proven to be very difficult.⁵

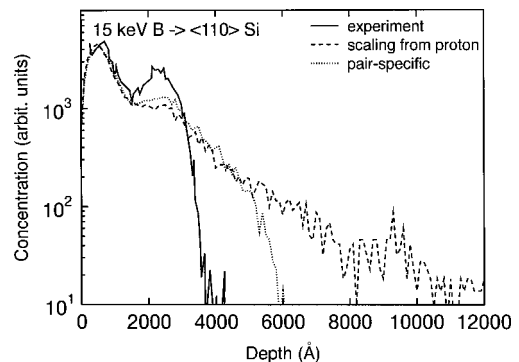


FIG. 2. Simulated and measured ranges of 15-keV B ions in the $\langle 110 \rangle$ channel of silicon (Ref. 28). The experimental data was measured with SIMS (Ref. 12).

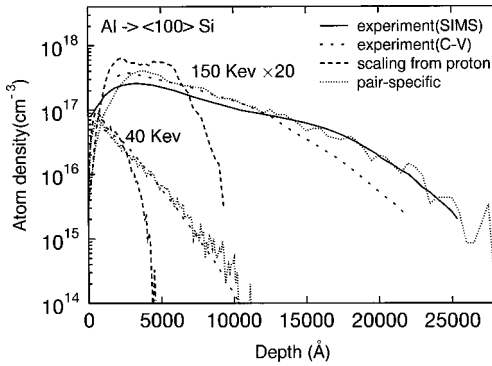


FIG. 3. Simulated and measured ranges of 40-keV and 150-keV Al ions in the $\langle 100 \rangle$ channel of silicon. The experimental data was measured with C - V in the 40-keV case and also with SIMS in the 150-keV case (Ref. 25). The ordinate in the figures is labeled “atom density” but for the C - V data this should actually be “active doping density.” The dimension for the two quantities is the same. The y scale for the 150-keV graphs is multiplied by 20 to make the picture clearer.

We have simulated 150-keV Al range distributions in all major channeling directions and our model was in all the cases in excellent agreement with the secondary-ion-mass spectroscopy (SIMS) data (see Figs. 3–5). For other energies in the relevant energy range we did not find any experimental SIMS data for channeling directions, but only capacitance-voltage (C - V) measurements.²⁵ In this method, the concentration of electrically active dopants in a semiconductor is obtained from a C - V measurement.²⁶ Although a C - V measurement only measures electrically active dopants, the fairly good agreement between the C - V and SIMS data at 150-keV indicates that the C - V data do give a reasonable estimate of the actual range profile. We obtained good agreement between our model and the C - V data at all the energies examined; results for 40 keV are shown in Figs. 3–5.

The figures also show that the pair-specific model is much better than the scaling-law model and gives excellent results for 40-keV and 150-keV cases in the $\langle 100 \rangle$ and $\langle 111 \rangle$ directions as well as a random direction (Fig. 6).

For P and As the simulations gave very good agreement with experiments in random directions for both models. In

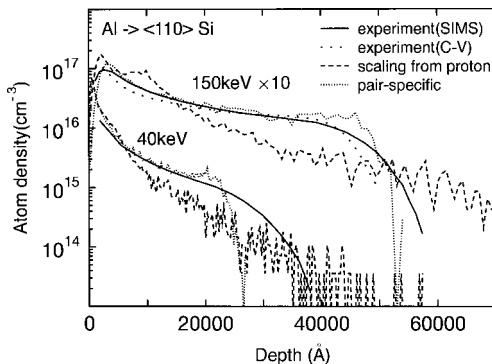


FIG. 4. As Fig. 3, but for the $\langle 110 \rangle$ channel (Ref. 28). The y scale for the 150-keV graphs is multiplied by 10 to make the picture clearer.

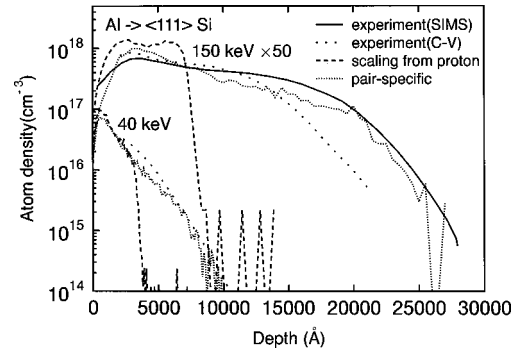


FIG. 5. As Fig. 3, but for the $\langle 111 \rangle$ channel. The y scale for the 150-keV graphs is multiplied by 50 to make the picture clearer.

the $\langle 100 \rangle$ and $\langle 111 \rangle$ directions the scaling-law model was found to somewhat underestimate the channeling, while the pair-specific one overestimates it by roughly the same amount. Sample data are shown in Figs. 7 and 8. It is not possible to state that one of these models would be better than the other. In the $\langle 110 \rangle$ channel agreement with experiments was not good for both P and As. Both models were found to overestimate ranges, although the pair-specific one was closer to the experimental values. Qualitatively the behavior was similar as that for B in the $\langle 110 \rangle$ channel (see Fig. 2).

The results presented here show that calculating ion ranges by the use of electronic stopping powers derived from pair-specific phase shift calculations gives good agreement with experimental range profiles in nonchanneling and most channeling directions in silicon, without the need for introducing any adjustable parameters. For protons the model has previously been demonstrated to work well.¹³ For the ion-target combinations B-Si, P-Si, and As-Si the agreement obtained with the current model is at least as good as that obtained with previous parameter-free models, while for Al-Si it is clearly better.

In all cases tested the present model works as well or better than any previous model with no free parameters. It is also noteworthy that except for the $\langle 110 \rangle$ channel, the model is of comparable quality with the best model which does employ one adjustable parameter.⁵

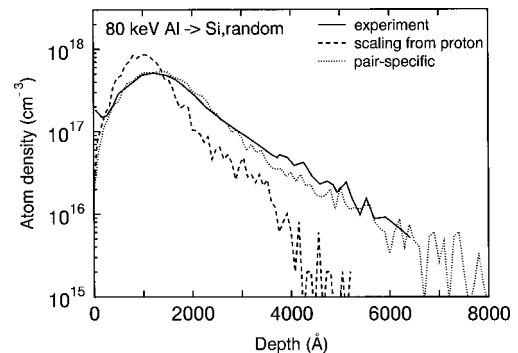


FIG. 6. Simulated and measured ranges of 80-keV Al ions in silicon ($\Theta = 7^\circ$, ϕ selected randomly). The experimental data were measured with SIMS (Ref. 29).

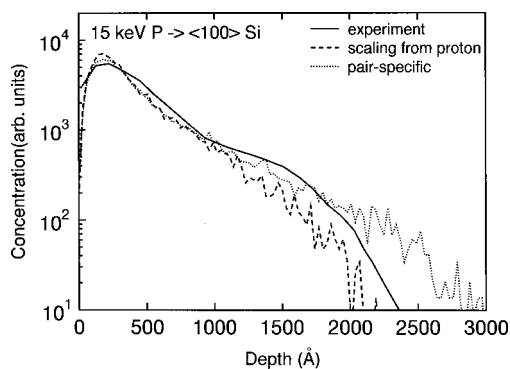


FIG. 7. Simulated and measured ranges of 15-keV P ions in the $\langle 100 \rangle$ channel of silicon. The experimental data was measured with SIMS (Ref. 12).

There is still some disagreement between the pair-specific model and experiments, however. The most serious problem appears to be that the tails of range profiles for P, As, and B implanted in the $\langle 110 \rangle$ channel are overestimated. However, the range profile is not seriously underestimated in any of the cases. This suggests that the remaining discrepancy could be explained by the lack of a charge averaging scheme in the model, as discussed in Ref. 13.

Although we have in this paper presented results only for the implantation into Si, mainly because of the scarcity of experimental data in other materials, the present approach can be used in any other material. It could be expected to work well at least in other tetrahedrally bonded semiconductor materials, like Ge and GaAs, while in other kinds of materials a somewhat different approach for obtaining the electronic stopping can be expected to be more accurate.²⁷

In conclusion, we have combined a molecular-dynamics range calculation method accounting accurately for nuclear

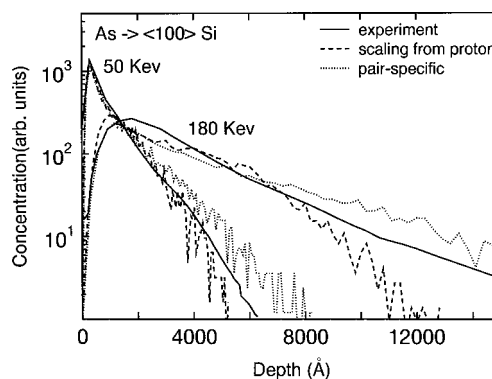


FIG. 8. Simulated and measured ranges of 50-keV and 180-keV As ions in the $\langle 100 \rangle$ channel of silicon. The experimental data were measured with SIMS (Ref. 12).

stopping with electronic stopping powers calculated using a three-dimensional electron charge distribution and phase shift factors derived from density-functional theory. Comparison of simulated and experimental range profiles for important dopants in channeling directions in Si showed that the model gives a reasonable description of at least B, P, Al, and As stopping in Si. Compared to other models with no adjustable parameters, the agreement with experiments is comparable to that of the best previous models for B, P, and As, and clearly better than previous models for Al ranges in Si.

We thank Professor N. Grønbech-Jensen and Dr. K. Beardmore for useful discussions. The research was supported by the Academy of Finland under Project No. 44215 and through its Center of Excellence Program (2000-2005). Grants of computer time from the Center for Scientific Computing in Espoo, Finland, are gratefully acknowledged.

*Present address: Department of Applied Science, University of California at Davis, Davis, California.

¹N. Bohr, *Philos. Mag.* **25**, 10 (1913).

²J. F. Ziegler, J. P. Biersack, and U. Littmark, *The Stopping and Range of Ions in Matter* (Pergamon, New York, 1985).

³D. F. Downey, C. M. Osburn, and S. D. Marcus, *Solid State Technol.* **40**, 71 (1997).

⁴K. Nordlund, J. Keinonen, and A. Kuronen, *Phys. Scr.* **T54**, 34 (1994).

⁵K. M. Beardmore and N. Grønbech-Jensen, *Phys. Rev. E* **57**, 7278 (1998).

⁶K. Nordlund, N. Runeberg, and D. Sundholm, *Nucl. Instrum. Methods Phys. Res. B* **132**, 45 (1997).

⁷J. Finneman, Ph.D. dissertation, The Institute of Physics, Aarhus, 1968.

⁸T. L. Ferrell and R. H. Ritchie, *Phys. Rev. B* **16**, 115 (1977).

⁹For a review, see R. O. Jones and O. Gunnarsson, *Rev. Mod. Phys.* **61**, 689 (1989).

¹⁰P. M. Echenique, R. M. Nieminen, and R. H. Ritchie, *Solid State Commun.* **37**, 779 (1981).

¹¹M. J. Puska and R. M. Nieminen, *Phys. Rev. B* **27**, 6121 (1983).

¹²D. Cai, N. Grønbech-Jensen, C. M. Snell, and K. M. Beardmore,

Phys. Rev. B **54**, 17 147 (1996).

¹³J. Sillanpää, K. Nordlund, and J. Keinonen, *Phys. Rev. B* **62**, 3109 (2000).

¹⁴J. Wang, J. Mathar, S. B. Trickey, and J. R. Sabin, *J. Phys.: Condens. Matter* **11**, 3973 (1999).

¹⁵W. Brandt and M. Kitagawa, *Phys. Rev. B* **25**, 5631 (1982).

¹⁶A. Mann and W. Brandt, *Phys. Rev. B* **24**, 4999 (1981).

¹⁷M. Deutsch, *Phys. Rev. B* **45**, 646 (1992).

¹⁸B. Dawson, *Proc. R. Soc. London, Ser. A* **298**, 379 (1967).

¹⁹R. F. Stewart, *J. Chem. Phys.* **58**, 1668 (1973).

²⁰N. K. Hansen and P. Coppens, *Acta Crystallogr., Sect. A: Cryst. Phys., Diffr., Theor. Gen. Crystallogr.* **A34**, 909 (1978).

²¹E. Clementi and C. Roetti, *At. Data Nucl. Data Tables* **14**, 177 (1974).

²²K. Nordlund, *Comput. Mater. Sci.* **3**, 448 (1995).

²³T. Schenkel, M. A. Briere, A. V. Barnes, A. V. Hamza, K. Bethge, K. Schmidt-Böcking, and D. H. Schneider, *Phys. Rev. Lett.* **79**, 2030 (1997).

²⁴J. P. Biersack and L. G. Hagmark, *Nucl. Instrum. Methods* **174**, 257 (1980).

²⁵R. Wilson and D. Jamba, *J. Appl. Phys.* **60**, 2806 (1986).

- ²⁶G. Dearnaley, J. H. Freeman, R. S. Nelson, and J. Stephen, *Ion Implantation* (North-Holland, Amsterdam, 1973).
- ²⁷J. Calera-Rubio, A. Gras-Martí, and N. R. Arista, Nucl. Instrum. Methods Phys. Res. B **93**, 137 (1994).
- ²⁸Following the sources of experimental data, we give the B ranges in the $\langle 110 \rangle$ channel as the projection to the $[001]$ axis, and the other $\langle 110 \rangle$ data in the direction of the channel.
- ²⁹G. Galvagno, A. Scandurra, V. Raineri, E. Rimini, A. L. Ferla, V. Sciascia, F. Frisina, M. Raspagliesi, and G. Ferla, Nucl. Instrum. Methods Phys. Res. B **74**, 105 (1993).